Targeting Hippocampal Phospholipid and Tryptophan Metabolism for Antidepressant-Like Effects of Albiflorin

Qiang-Song Wang , Kuo Yan , Kuang-Dai Li , Li-Na Gao , Xu Wang , Haibo Liu , Zuoguang Zhang , Kefeng Li , Yuan-Lu Cui

PII: S0944-7113(21)00278-6
DOI: https://doi.org/10.1016/j.phymed.2021.153735
Reference: PHYMED 153735

To appear in: *Phytomedicine*

Received date: 28 April 2021
Revised date: 31 July 2021
Accepted date: 5 September 2021

Please cite this article as: Qiang-Song Wang , Kuo Yan , Kuang-Dai Li , Li-Na Gao , Xu Wang , Haibo Liu , Zuoguang Zhang , Kefeng Li , Yuan-Lu Cui , Targeting Hippocampal Phospholipid and Tryptophan Metabolism for Antidepressant-Like Effects of Albiflorin, *Phytomedicine* (2021), doi: https://doi.org/10.1016/j.phymed.2021.153735

For Submission to Phytomedicine

Targeting Hippocampal Phospholipid and Tryptophan Metabolism for Antidepressant-Like Effects of Albiflorin

Qiang-Song Wang[a], Kuo Yan[b], Kuang-Dai Li[b], Li-Na Gao[b], Xu Wang[c], Haibo Liu[d], Zuoguang Zhang[e], Kefeng Li[f,*], Yuan-Lu Cui[b,**]

[a] Institute of Biomedical Engineering, Chinese Academy of Medical Sciences & Peking Union Medical College, Tianjin, 300192, China

[b] Research Center of Traditional Chinese Medicine, Tianjin University of Traditional Chinese Medicine, Tianjin, 301617, China

[c] State Key Laboratory of Food Nutrition and Safety, College of Food Engineering and Biotechnology, Tianjin University of Science and Technology, Tianjin, 300457, China

[d] Institute of Medicinal Plant Development, Chinese Academy of Medical Sciences & Peking Union Medical College, Beijing, 100193, China

[e] Beijing Wonner Biotech. Co. Ltd., Beijing, 101111, China

[f] School of Medicine, University of California, San Diego, San Diego, CA, 92093, USA

Correspondence: *Kefeng Li: School of Medicine, University of California, San Diego, 9500 Gilman Dr, La Jolla, CA, 92093, USA.

**Yuan-Lu Cui: Research Center of Traditional Chinese Medicine, Tianjin University of Traditional Chinese Medicine, 10 Poyang Lake Road, West Zone of Tuanbo New City, Jinghai District, Tianjin, 301617, China.

E-mail addresses: kli@ucsd.edu (K. Li), cuiyl@tju.edu.cn (Y-L. Cui)

Highlights

- Current antidepressants showed delayed onset and limited therapeutic efficacy.
- Albiflorin produces antidepressant-like effects in three models of depression.
- The effects of albiflorin are associated with phospholipid and tryptophan metabolism.
- Albiflorin inhibits cPLA2 in hippocampal phospholipid metabolism.
- Albiflorin corrects tryptophan metabolism via the cPLA2- Akt1-IDO1 regulatory loop.

Graphical abstract

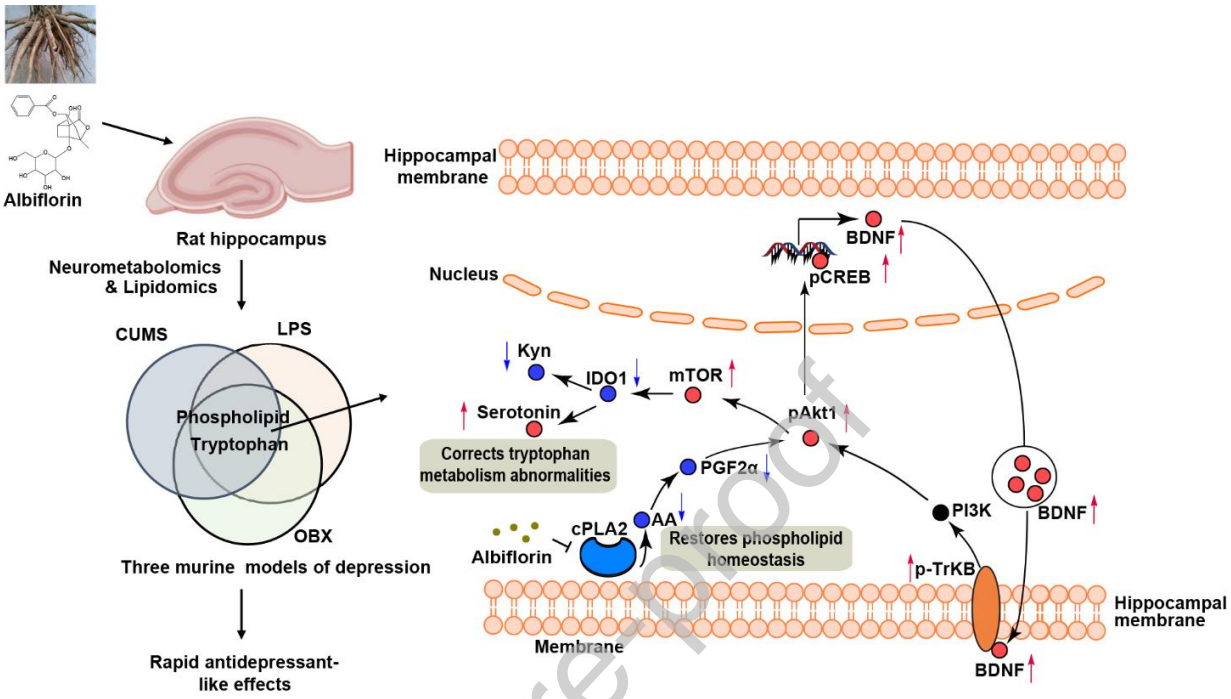

Abstract

Background: Current antidepressant therapy remains unsatisfactory due to its delayed clinical onset of action and the heterogeneity of depression. Targeting disturbed neurometabolic pathways could provide a novel therapeutic approach for the treatment of depression. Albiflorin is a phytomedicine isolated from the roots of Peony (*Paeonia albiflora* Pall) with excellent clinical tolerance. Until now, the antidepressant-like activities of albiflorin in different subtypes of depression and its effects on neurometabolism are unknown.

Purpose: The objective of this study was to investigate the rapid antidepressant-like effects of albiflorin in three common animal models of depression and elucidate the pharmaco-metabolic mechanisms of its action using a multi-omics approach.

Results: We found that albiflorin produces rapid antidepressant-like effects in chronic unpredictable mild stress (CUMS), olfactory bulbectomy (OBX), and lipopolysaccharide (LPS)-induced murine models of depression. Using a system-wide approach combining metabolomics, lipidomics, and transcriptomics, we showed that the therapeutic effects of albiflorin are highly

associated with the rapid restoration of a set of common metabolic abnormities in the hippocampus across all three depression models, including phospholipid and tryptophan metabolism. Further mechanistic analysis revealed that albiflorin normalized the metabolic dysregulation in phospholipid metabolism by suppressing hippocampal cytosolic phospholipases A2 (cPLA2). Additionally, inhibition of cPLA2 overexpression by albiflorin corrects abnormal kynurenine pathway of tryptophan metabolism via the cPLA2-protein kinase B (Akt1)-indoleamine 2,3-dioxygenase 1(IDO1) regulatory loop and directs tryptophan catabolism towards more hippocampal serotonin biosynthesis.

Conclusion: Our study contributed to a better understanding of the homogeneity in the metabolic mechanisms of depression and established a proof-of-concept for rapid treatment of depression through targeting dysregulated neurometabolic pathways.

Keywords: Antidepressant-like effects; Albiflorin; Hippocampus; Neurometabolism

Abbreviations

3-HK, 3-hydroxykynurenine; AEA, Anandamide; Akt1B, Protein kinase B; Alb, Albiflorin; BBB, Blood-brain-barrier; BDNF, Brain-derived neurotrophic factor; Cer, Ceramide; COX-2, Cyclooxygenase-2; cPLA2, Cytosolic phospholipases A2; CUMS, Chronic unpredictable mild stress; DEGs, Differentially expressed genes; ETV4, ETS translocation variant 4; Flx, Fluoxetine hydrochloride; GSK, Glycogen synthase kinase 3 ; I.G., Intragastric gavage; IDO1, Indoleamine 2,3-dioxygenase 1; Imh, Imipramine hydrochloride; Kyn, Kynurenine; LC-MS/MS, Liquid chromatography with tandem mass spectrometry; LOOCV, Leave-one-out cross-validation; LPS, Lipopolysaccharide; MDD, Major depressive disorder ; MRM, Multiple reaction monitoring; MWAS, Metabolome-wide association study; NAPE-PLD, N-acyl phosphatidylethanolamine phospholipase D; NSAIDs, Nonsteroidal anti-inflammatory drugs; OBX, Olfactory bulbectomy; OFT, Open-field test; PA, Phosphatidic acid; PC, Phosphatidylcholine; PCNA, Proliferating cell nuclear antigen; PE, Phosphatidylethanolamine; PI, Phosphatidylinositol; PI3K, Phosphatidylinositol 3 kinase; PIsEtn, Ethanolamine plasmalogens; PKC, Protein kinase C; PLS-DA, Partial least-squares discriminant analysis; QUIN, Quinolinic acid; Sal, Saline; SM, Sphingomyelin; TCM, Traditional Chinese Medicine; TEM, Transmission electron microscopy; TST, Tail suspension test; VIP, Variable importance in the projection

Introduction

Depression is one of the most common psychiatric disorders affecting over 320 million people worldwide (Friedrich, 2017). It is also the second leading cause of disability and a major contributor to the burden of suicide (Murray and Lopez, 1997). The number of patients with depression is expected to increase substantially in post-COVID-19 era and one-third of COVID-19 survivors had persistent neurocognitive impairment (Li et al., 2020; Li et al., 2021; Mazza et al., 2021). Depression is a rather complicated and heterogeneous disorder (Drysdale et al., 2017). The cardinal symptoms of depression include depressed mood, cognitive impairment, and anhedonia (Belmaker and Agam, 2008). In addition, inflammation is the prevalent comorbidities in patients with major depressive disorder (MDD) (Dantzer et al., 2008; de Bodinat et al., 2010; Vuong et al., 2017). Current antidepressant therapy remains unsatisfactory because of its delayed clinical onset, limited therapeutic efficacy, and undesirable side effects (Berton and Nestler, 2006; Harmer et al., 2017; Zhang et al., 2020). Although some patients show partial responses within 2 weeks, classical antidepressants usually require several weeks to reach full effectiveness, and nearly 50% of patients do not respond to the first medication prescribed (Duman et al., 2016).

Natural products have been a rich reservoir of new drugs or drug leads due to their vast structural diversity with biological relevance (van Hattum and Waldmann, 2014). It was estimated that 34% of FDA approved small molecule drugs between 1981 and 2010 were natural products or their derivatives (Harvey et al., 2015). The majority of these natural product-derived drugs are anticancer and antimicrobial agents such as artemisinin, trabectedin, and romidepsin (Mishra and Tiwari, 2011). There are few natural products in the fields of neurology and psychiatry. Recent metabolomic studies have dramatically expanded our understanding of the pathophysiology of depression and highlighted the role of metabolic disturbances in the pathogenesis of depression (Pu et al., 2020). Moreover, rats and human beings share an

overwhelming majority of their biochemical metabolism (Blais et al., 2017). Therefore, preclinical drug development based on metabolic pathways in rats could be much easier to be transferred to humans.

Peony (*Paeonia albiflora* Pall) is an ornamental plant native to Asia, Europe, and Northern America. The dry root of Peony has been prescribed for more than 1000 years in Traditional Chinese Medicine (TCM) with excellent clinical tolerance for the treatment of rheumatoid arthritis (He and Dai, 2011). Albiflorin (Fig. 1A) is one of the main bioactive compounds in Peony roots. Long-term treatment with albiflorin produced the antidepressant-like effects on a chronic unpredictable mild stress (CUMS) model of depression (Wang et al., 2016). Moreover, in our previous work, we evaluated the toxicity of albiflorin using both the FDA preclinical protocol and next generation metabolomic approach and no obvious acute oral toxicity was observed for both the rat and dog models (maximum tolerated dose > 5000 mg/kg for Beagle dogs and no-observed-adverse-effect level of 450 mg/kg for SD rats) (Han et al., 2018). All these suggested the potential use of albiflorin as an effective and safe antidepressant. However, the molecular mechanisms underlying the antidepressant-like effects of albiflorin are largely unknown. It was reported that albiflorin had no significant affinity to a wide range of central nervous system receptors, including receptors for dopamine (D1-D5), serotonin, norepinephrine, acetylcholine (M1-M5), opioids, adenosine (A1, A2A) and histamine (H1-H4) (Jin et al., 2016). A recent report also showed that the gut microbiome might play a causal role in regulating the antidepressant-like efficacy of albiflorin (Zhao et al., 2018).

In this study, we evaluated the rapid antidepressant-like effects of albiflorin using three representative rodent models of depression, including olfactory bulbectomy (OBX), CUMS, and lipopolysaccharide (LPS) induced depressive-like behaviors. We investigated the mechanisms of action of albiflorin using system-wide approaches combining metabolomics and transcriptomics followed by transmission electron microscopy (TEM) imaging, molecular docking,

and targeted lipidomic analysis validation. Overall, our results provide an important stepping-stone for the translation of exciting advances in treating depressive-like behaviors using albiflorin in rats into clinical therapies.

Materials and Methods

The brief materials and procedures were summarized here, and the additional details were described in the supplemental materials.

Animals and drugs

All animal experiments were conducted in accordance with the protocols approved by the Institutional Animal Care and Use Committee of Tianjin University of Traditional Chinese Medicine on March 7, 2014 (Approval no. TCM-2014-037-E15). Male ICR mice (22 - 24 g), male Sprague Dawley (SD) rats (6-7-week-old, 180 - 220 g) and male C57BL/6J mice (8-week-old, 20 - 22 g) were purchased from Beijing Huafukang Bioscience Co. Ltd. Male Wistar rats (6-7-week-old, 180 - 220 g) were obtained from the Laboratory Animal Center of the Academy of Military Medical Sciences. Animals were housed under controlled temperature (22 - 24 ºC), humidity (40 - 60%), and 12 h light/dark cycles with ad libitum food and water before the experiments. Albiflorin was provided by Beijing Wonner Biotech (Purity > 95%). Fluoxetine hydrochloride (Prozac) and duloxetine hydrochloride were purchased from Eli Lilly and Company. Imipramine hydrochloride (Imh) was bought from Sigma Aldrich. Albiflorin, fluoxetine, and duloxetine were dissolved in sterile 0.9% saline solution and stored at 4 ºC for up to 48 h. Ketamine hydrochloride injection was purchased from Fujian Gutian Pharmaceutical Co., Ltd (Fujian, China).

The antidepressant potential of albiflorin

The antidepressant potential of albiflorin was assessed by tail suspension test (TST) in male SD rats. Briefly, rats were randomly divided into 3 groups (12 mice/group) and administrated with either 0.9% saline (Sal), fluoxetine (10 mg/kg), or three different doses of albiflorin (3.5, 7, and 14 mg/kg) via intragastric gavage (I.G.). TST was performed 1 h after drug administration.

Effect of albiflorin on the spontaneous locomotor activity in rats

To exclude nonspecific effects of albiflorin, the spontaneous locomotor activity of mice was evaluated in the open-field test (OFT). The group set up and drug administration were the same as described in the previous section. OFT was conducted 1 h after drug administration. The animals were individually placed in a black box (50 × 50 × 40 cm). The moving distance of the mice was recorded by an automated tracking system (Ethovision, The Netherlands) connected to video camera positioned overhead. The total distance traveled during the last 5 min of the 6-min test was the indicator of locomotor activity.

OBX model of depression

Male Wistar rats were anesthetized with chloral hydrate (400 mg/kg, I.P.), and the olfactory bulbs were removed as described in the supplemental materials. Sham animals were treated identically with the exception that the olfactory bulbs were left intact. After 14 days' recovery, rats were then blindly randomized into groups (12 rats/group) and treated daily for 7 days with either saline, Imh or albiflorin via I.G.: Sham-Sal (Sham rats with saline); OBX-Sal (OBX rats with saline); OBX-Imh (OBX rats with Imh, 5 mg/kg body weight) and OBX-Alb (OBX rats with Alb, 3.5, 7 and 14 mg/kg body weight). OFT was conducted to assess the locomotor activity after drug administration. The total distance traveled by each animal over a 3 min period was measured.

LPS-induced depressive-like behaviors

The generation of LPS-induced depressive-like behavior in mice was performed as described before (Lee et al., 2018). Briefly, male C57BL/6J mice were randomly allocated into six groups with 12 per group: Ctrl-Sal (Control with saline), LPS-Sal (LPS with saline), LPS-Flx (LPS with Flx, 10 mg/kg body weight) and LPS-Alb (LPS with Alb, 3.5, 7 and 14 mg/kg body weight). Dosing of all drugs began on day 1 and continued once daily for 7 days via I.G. After the final dosing at day 7, LPS (0.83 mg/kg) or saline was administrated intraperitoneally. OFT and FST were conducted at 24 h after LPS administration. The heparinized plasma was collected after drug treatment. The animals were then sacrificed, and the hippocampi were collected and stored in liquid nitrogen for further analysis.

CUMS model of depression

Male SD rats were randomly assigned to the control or CUMS group. Rats in the CUMS group were exposed to one random stressor per day for 35 days (Details in the supplemental materials). Following 4 weeks of stress exposure, rats with stress-induced depression-like behaviors were used for drug treatment.

Single-dose treatment: CUMS rats were treated with either a single dose of albiflorin (CUMS-Alb, 7 mg/kg body weight, I.G.), ketamine (CUMS-Ket, 10 mg/kg body weight, I.P.), or saline (CUMS-Sal). Control rats without stress were given saline (Ctrl-Sal). Eight rats were used per group. Sucrose preference test (SPT) was performed once a week and 24 h after drug treatment. The consumption amount of total water and 1% sucrose were measured by weighing the bottles before and after the test. The sucrose preference was then calculated according to the following equation:

$$\text{Sucrose preference (\%)} = \frac{\text{Sucrose intake (g)}}{\text{Sucrose intake + water intake (g)}} \times 100\%$$

OFT was conducted before and 24 h after drug treatment. The number of crossings and rearings during a 4-min period was counted.

Treatment for 7 days: CUMS rats were given either albiflorin (CUMS-Alb, 3.5, 7 and 14 mg/kg body weight), fluoxetine (CUMS-Flx, 10 mg/kg body weight), or saline (CUMS-Sal) for 7 days via I.G. Control rats without stress were given saline (Ctrl-Sal). Eight rats were used per group. Behavior tests were the same as the description in the single-dose treatment. Rat heparinized plasma was collected after drug treatment. The animals were then sacrificed, and the hippocampi were collected. The whole procedures were repeated three times including the generation and validation of CUMS model of depression, drug treatment and behavior tests. The plasma and hippocampi samples were combined and snap-frozen in liquid nitrogen for further analysis.

Western blot analysis

Rat hippocampal tissues from the animal experiments of LPS-induced depressive-like model and CUMS model of depression were used for western blot analysis. Total protein from rat hippocampi was extracted and quantified. Sixty micrograms of total protein were resolved on 10% SDS-PAGE gels and probed by using primary antibodies. The antibodies, their sources, and catalog numbers were listed in Table S5. Three independent experiments were performed.

H&E staining and immunohistochemistry

For H&E staining, tissues obtained from rats in the animal experiment of CUMS model of depression were fixed with a mixture of 2% formalin and 2% glutaraldehyde solution. The tissues were then paraffin-embedded, cut into 4-μm thick sections, and fixed on glass slides. The slides were deparaffinized, rehydrated, stained with hematoxylin (5 min) and eosin (30 s). After staining, the sections were dehydrated through increasing concentrations of ethanol and xylene. The slides were examined, and the images were captured using a LEICA DM4000B

microscope (Leica, Germany). For immunostaining, the slides were incubated with anti-PCNA (1:100 dilution) overnight at 4 °C and then secondary antibody anti-rabbit IgG. The number of positive cells was counted using a Nikon Eclipse Ti-U inverted fluorescent microscope (Nikon, Japan).

Pharmacokinetic (PK) analysis of albiflorin

Albiflorin was given to CUMS rats via I.G. at the dose of 7 mg/kg body weight. Blood was taken at 0.083, 0.25, 0.5, 0.75, 1, 2, 3, 4, 6, 8, 12 and 24 h after drug administration. Each time point has 8 rats. The animals were sacrificed after blood collection at each time point, and the hippocampus was collected. Albiflorin in the plasma and the hippocampus was extracted, and the concentration was analyzed using LC-MS/MS (Details in the supplemental materials). Geniposide was used as the internal standard. Non-compartmental pharmacokinetic parameters were calculated by Kinetica 5 (Adept Scientific, UK), including C_{max}, $T_{max,}$ $t_{1/2(h),}$ $AUC_{last,}$ and mean residence time (MRT).

Metabolomic analysis

Metabolite extraction from plasma and hippocampal tissues was performed as described with minor changes (Yuan et al., 2012). Eight replicates were used per group. The metabolomic analysis was performed on a Waters ACQUITY UPLC coupled with a QTRAP 6500 MS/MS system (SCIEX, USA) as described before (Yuan et al., 2012). Ten microliters of the extract were injected into a Luna NH_2 aminopropyl HPLC column (250 × 2 mm, 3 μm, Phenomenex, USA) held at 25 °C for chromatographic separation. A total of 482 metabolites covering all the major metabolic pathways were targeted by scheduled multiple reaction monitoring (MRM) under Analyst v1.6.2 software control in both negative and positive mode with rapid polarity switching (20 ms) (Li et al., 2014; Yuan et al., 2012). The chromatographic peaks were inspected and integrated using MultiQuant 3.0 (SCIEX, USA). The pooled plasma and

hippocampal samples were used as quality control (QC) and injected 3 times in each batch to monitor MS signal drift.

RNA sequencing

RNA sequencing was performed by Beijing Novogene Technology Co. Ltd. Total RNA was extracted from rat hippocampi (4 replicates/group) with TRIzol (Invitrogen, USA). Sequencing libraries were prepared using NEBNext Ultra RNA Library Prep Kit. The library preparations were sequenced on a HiSeq 2500 platform (Illumina, USA). Details for data processing were described in the supplemental materials.

Transmission electron microscopy (TEM)

Rat hippocampal samples were fixed in 4% paraformaldehyde (PFA) and 2.5% glutaraldehyde, dehydrated in an ascending ethanol series, and embedded in Epon/Araldite resin. Ultra-thin (60 nm) sections were cut using a Leica EM UC7 ultramicrotome (Leica Microsystems, Wetzlar, Germany) and counterstained with uranyl acetate and Reynolds lead citrate (Leica Microsystems, Wetzlar, Germany). The sections were then examined at 120 kV using a Hitachi H-7650 transmission electron microscope (Hitachi, Tokyo, Japan). High-resolution montages (4 × 4 montages at 2 k× or 15 k× magnification) were captured for randomly selected neurons. Four groups (Ctrl-Sal, CUMS-Sal, CUMS-Flx, and CUMS-Alb) with two samples per group were prepared. The montages were recorded using an AMT XR-41 camera (4 megapixels) (Advanced Microscopy Techniques, MA).

Lipidomic analysis

Lipids in the extract were analyzed using a Waters ACQUITY UPLC system coupled with a QTRAP 6500 mass spectrometer (SCIEX, USA) according to our previous study with modifications (Cui et al., 2017; Shi et al., 2018). Individual lipid species were measured by MRM transitions. The major membrane lipids including phosphatidylcholine (PC),

phosphatidylethanolamine (PE), phosphatidylinositol (PI), phosphatidic acid (PA), sphingomyelin (SM), ceramide (Cer), and cholesterol were targeted. Lipid concentration was calculated by reference to appropriate internal standards.

Targeted analysis of tryptophan metabolism by liquid chromatography with tandem mass spectrometry (LC-MS/MS)

The concentrations of hippocampal metabolites in tryptophan metabolism were also confirmed using a different analytical method by LC-MS/MS. Eight replicates were used per group. The following multiple reaction monitoring (MRM) transitions (Q1/Q3) were used for quantification: tryptophan (205/146), kynurenine (209.1/94), 3-hydroxykynurenine (225.2/208.3), serotonin (177.1/160), melatonin (233.1/174.1) and quinolinic acid (168/149.9), tryptophan-$^{13}C_{11}$ (216/155), kynurenine-$^{13}C_{10}$ (219.1/202), melatonin-d_4 (237.1/178.1), serotonin-d_4 (181.1/164.1), 3-hydroxykynurenine-$^{13}C_{10}$ (235.2/218) and quinolinic acid-$^{13}C_7$ (175/157). The absolute concentration was calculated using the corresponding internal stable isotope standards.

Molecular docking analysis of albiflorin

The docking experiment was performed using MOE 2016 (Chemical computing group, Canada) to explore the interaction between albiflorin and the key enzymes in phospholipid metabolism including cytosolic phospholipases A2 (cPLA2), cyclooxygenase-2 (COX-2), Sphingosine kinase 1 (Sphk1), Glycogen synthase kinase 3ß (GSK3ß), and indoleamine 2,3-dioxygenase (IDO1). The best docking result was judged by comprehensive analysis, comparison, and energetic considerations. After that, further refinement was carried on the best results. The residues within 6 Å from the ligand were set to be flexible. Energy minimization was carried out by conjugated gradient minimization with the MMFF94x force field until an RMSD of 0.1 kcal mol^{-1} $Å^{-1}$ was achieved. Finally, a 5 ns molecular dynamics simulation was conducted to confirm the stability of the binding modes.

In vitro enzymatic assay for cPLA2 and IDO1 inhibition

In vitro enzymatic assay for the inhibition of cPLA2 activity by albiflorin was performed using the cPLA2 assay kit obtained from Cayman Chemical according to the manufacture's protocol (Ann Arbor, Michigan, USA). Arachidonyl trifluoromethyl ketone (ATK), a known cPLA2 inhibitor was used as the positive control. Different concentrations of albiflorin were tested with three replicates for each concentration and the level of albiflorin required for 50% inhibition of cPLA2 (IC_{50}) was determined.

In vitro enzymatic assay for IDO1 inhibition was conducted using Ehrlich's reagent. Triplicates were prepared for each concentration. The IDO1 activity was determined by measuring the absorption of the reaction product at 480 nm. The level of albiflorin required for 50% inhibition of IDO1 compared to the negative controls (IC_{50}) was determined. NLG919, a known IDO1 inhibitor, was used as the positive control.

Statistical analysis

Details for analysis of omic data were described in the supplementary materials. Briefly, for metabolomic analysis, data were log2 transformed and normalized by auto-scaling prior to the statistical analysis. Multivariate analysis (Partial least-squares discriminant analysis, PLS-DA) and pathway enrichment analysis were performed using Metaboanalyst 4.0. Since PLS-DA is a supervised model, leave-one-out cross-validation (LOOCV) and permutation test were performed to avoid overfitting. Metabolites driving the differences were identified based on variable importance in the projection (VIP). VIP score > 1.5 was considered significant. Univariate analysis was used to validate the results of VIP analysis. Kendall rank correlation was conducted to explore the metabolome-wide associations between the differential metabolites and the improvement of depressive-like behaviors after albiflorin treatment. The cut-off values were $P < 0.05$ and coefficient $r > 0.5$ or < -0.5. Pathway analysis was performed

against a pathway library of *Rattus norvegicus* (total 81 pathways). *P* value was calculated by Fisher's exact test. The integration of metabolomic and transcriptomic data was conducted using MetScape 3.1, a plug-in to Cytoscape 3.8.0.

Other statistical analyses were performed using Prism 8.0 (GraphPad, CA) or R 4.0.3. Data were mean ± standard error of the mean (SEM) or standard deviation (SD) described in the legends. Depending on the data distribution, either a two-tailed *t*-test or Mann-Whitney test was used to calculate significance levels between the two groups. One-way ANOVA (parametric) followed by Post hoc Tukey's or Kruskal-Wallis (nonparametric) was used to compare multiple groups. $P < 0.05$ was considered statistically significant.

Results

Albiflorin produces fast-onset antidepressant-like effects in three murine models of depression

We followed a recently recommended systematic approach for assessment and validation of the rapid antidepressant-like activity of albiflorin (Ramaker and Dulawa, 2017). We first evaluated the antidepressant-like potential of albiflorin using three doses (3.5, 7, and 14 mg/kg). As shown in Fig. 1B, rat treated with albiflorin showed a significant decrease of TST immobility time in a dose-dependent manner from 3.5 to 7 mg/kg (Fig. 1B). There was no statistical difference between 7 and 14 mg/kg (Fig. 1B). To exclude the inhibitory or excitatory effects of albiflorin, we examined the spontaneous locomotor activity of mice in the OFT. Rat treated with three different doses of albiflorin had no significant changes in the total distance traveled within 5 min (Fig. 1C). These results indicated that albiflorin did not alter the psychomotor and exploratory activity of the animals. We then used 7 mg/kg of albiflorin for the following experiments.

We next examined the effects of albiflorin in three murine models covering the major symptoms of depression in humans: LPS-induced depressive behaviors, OBX, and CUMS. We found that LPS injection resulted in a significant reduction in the number of rearings (Fig. 1D) and total distance traveled in OFT (Fig. S1A). This depressive-like hypolocomotion in mice was normalized by albiflorin (Fig. 1D and Fig. S1A). In addition, albiflorin completely corrected the increased time of immobility in mice caused by LPS in FST (Fig. S1B).OBX mimics motor agitation and is one of the most reliable and sensitive tests to predict the time of antidepressant onset accurately (Ramaker and Dulawa, 2017). As shown in Fig. 1E, OBX-induced hyperactivity in rats was completely normalized after 7 days of albiflorin treatment but not imipramine in OFT. In the CUMS model, generally, CUMS-induced anhedonia is not normalized by subchronic treatment with classical antidepressants (Ramaker and Dulawa, 2017). In this study, we demonstrated that a single dose of either ketamine (10 mg/kg) or albiflorin (7 mg/kg) completely reversed the reduction of sucrose intake in rats with chronic stress (Fig. 1F). No statistical difference was observed between ketamine and albiflorin (Fig. 1F). Similar to ketamine, a single dose of albiflorin corrected the reduction of rearings in rats caused by CUMS (Fig. 1G). Furthermore, albiflorin exerted a more potent anti-anhedonia effect than fluoxetine (Fig. 1H). Fluoxetine treatment for 7 days only slightly increased the sucrose preference without a significant difference from the untreated CUMS rats ($P > 0.05$, Fig. 1H). Additionally, the chronic stress-induced decrease of rearings in OFT was normalized by 7 days of albiflorin treatment (Fig.1I).

The expression of brain-derived neurotrophic factor (BDNF), and the phosphorylation of CREB (Ser 133), and TrKB in the hippocampus are hallmark events of antidepressant onset (Ramaker and Dulawa, 2017). We next analyzed whether albiflorin could rapidly upregulate the expression of these proteins. With traditional antidepressants, the upregulation of BDNF-TrKB signaling requires 14-21 days of treatment (Duman and Voleti, 2012). Interestingly, we found that 7 days of albiflorin treatment led to a significant upregulation of BDNF expression and the

increase of TrKB phosphorylation (pTrKB/TrKB) in the hippocampus compared to the stressed rats received saline (Fig. 1J, and 1K). In contrast, BDNF following 7 days of fluoxetine treatment were not significantly different from the stressed rats received saline. In addition, the pCREB/CREB ratio was significantly upregulated with albiflorin administration for 7 days (Fig. 1L), while there was only a nonsignificant trend of increase for fluoxetine treatment compared to the stressed rats received saline (Fig. 1L).

We next examined the histopathological changes of the hippocampus in response to chronic stress and albiflorin treatment. Fig. 1M – 1N showed that the number of proliferating cell nuclear antigen (PCNA)-positive cells was decreased after chronic stress. However, animals treated with albiflorin had significant improvement in cell survival, indicated by the presence of more PCNA-positive cells (Fig. 1O - 1P). Similarly, from H&E staining, we observed dramatic damage of pyramidal cells with disorganized layers in the hippocampal CA3 region in response to chronic stress (Fig. S2). These abnormalities were rapidly reversed by albiflorin administration (Fig. S2).

Previous studies had shown that albiflorin could penetrate blood-brain-barrier (BBB) in both normal rats and rats with ischemia/reperfusion (I/R) (Hu et al., 2016; Li et al., 2015). In this study, we analyzed the pharmacokinetic actions of albiflorin in CUMS rat plasma and hippocampi. Surprisingly, we found that albiflorin was detectable in rat plasma and hippocampi as soon as 5 min following I.G. administration (Fig. S3A and S3B). Albiflorin reached the peak concentration in rat plasma at 30 min and hippocampi at 45 min post-administration (Fig. S3C and S3D). Overall, our data suggested that albiflorin could enter the hippocampus and produces antidepressant-like effects. We next applied a systematic, integrated multi-omics approach to explore the pharmcomechanisms of antidepressant-like actions for albiflorin.

The rapid antidepressant-like actions produced by albiflorin is highly associated with the correction of metabolic dysregulation in hippocampal phospholipid and tryptophan metabolism in three depression models

We first compared the changes in hippocampal metabolism of three depression models using both metabolomic and lipidomic approaches. We found 11 metabolic pathways were significantly disturbed in OBX and CUMS models of depression, and 12 pathways were altered in the LPS model compared to the normal controls (Table S1 - S3). The Venn diagram of differential metabolic pathways in common or unique to the three depression models is shown in Fig. 2A. We identified four metabolic pathways that were overlapped in all three depression models, including phospholipid, arachidonic acid, tryptophan metabolism, and TCA cycle (Fig. 2A).

To understand the mechanisms of action of albiflorin, we next examined the metabolic changes and gene expression alternations in the hippocampus of CUMS rats after albiflorin treatment using metabolomics, lipidomics, and RNA sequencing. Multivariate analysis of metabolomic data with PLS-DA showed that both a single dose of ketamine (CUMS-Ket) and albiflorin (CUMS-Alb) led to the complete separation of their metabolite profiles in the hippocampi from saline-treated CUMS rats (CUMS-Sal) (Fig. 2B and 2C). Compared to the ketamine-treated group, the dots of the albiflorin-treated group were closer and partially overlapped to the dots of the control group (Ctrl-Sal). The reliability of the PLS-DA model was further validated using the LOOCV approach with q^2 values > 0.4 (Fig. S4A). This suggested that albiflorin has more potency to improve the disturbed metabolic abnormalities after chronic stress than ketamine. Consistently, a distinct separation of hippocampal metabolite profiles was observed between CUMS rats treated 7 days of albiflorin and saline-treated group (Fig. 2D). In contrast, fluoxetine treatment only showed partial separation of hippocampal metabolomic profiles from CUMS rats treated with saline (Fig. 2E). LOOCV analysis confirmed the reliability

of the PLS-DA model separation of different groups (Fig. S4B). Volcano plot analysis showed that albiflorin significantly changed more metabolites than fluoxetine in both the hippocampus and plasma (Fig. S5A and S5B). Similar to the metabolomic results, transcriptomic analysis of global gene expression in the hippocampus showed that albiflorin altered the expression of many more transcripts compared to fluoxetine treatment (Fig. S5C and S5D). Compared with CUMS rats treated with saline (CUMS-Sal), the expression of 415 transcripts in rat hippocampi was dramatically changed in response to albiflorin treatment (CUMS-Alb) while only 219 in the fluoxetine group (CUMS-Flx) with 112 common ones in both groups (Fig. 2E).

We then integrated the metabolomic and transcriptomic data to identify the metabolic pathways and molecular interactions changed in rat hippocampus in response to albiflorin treatment. A total of 132 metabolite discriminators and 415 differentially expressed genes (DEGs) were used for pathway network analysis. We found that albiflorin treatment triggered dramatic pharmaco-metabolic changes in rat hippocampus (Fig. 2G). Pathway enrichment analysis of plasma metabolomic data showed similar metabolic pathways altered by albiflorin treatment (Fig. S6). Among the abnormal metabolic pathways restored by albiflorin, the most dramatic effects were the correction of abnormal phospholipid metabolism, followed by tryptophan metabolism (Table S4).

Additionally, we conducted a metabolome-wide association study (MWAS) to investigate the hippocampal metabolites correlated with the improvement of depressive-like behaviors after albiflorin treatment. Fig. 2H and Fig. 2I list the top 20 hippocampal metabolites significantly associated with the increase of locomotor activities in response to albiflorin treatment. This MWAS analysis further confirmed that albiflorin produces rapid antidepressant-like effects by correction of metabolic abnormalities in phospholipid and tryptophan metabolism in the hippocampus. We next focused on illustrating how albiflorin restores abnormal hippocampal phospholipid and tryptophan metabolism, which are commonly disturbed in all three murine models of depression tested in this study.

Albiflorin restores dysregulated hippocampal phospholipid metabolism via inhibiting cPLA2

To further assess the effects of albiflorin on neuronal phospholipid membrane in rat hippocampi, we performed TEM analysis of membrane lipids arrangement in hippocampal cells. As shown in Fig. 3A, the control group without stress (Ctrl-Sal) have intact cell membrane and lipid bilayers (See the structures marked with arrows). The cellular integrity of hippocampal cells was lost after 4 weeks of chronic stress (CUMS-Sal, Fig. 3A). Their cell membranes and lipid bilayers were severely damaged. Albiflorin treatment rapidly restored the structural integrity of the lipid bilayers, while some cells with damaged cell membranes were still present in the fluoxetine-treated group (Fig. 3A, see the arrows in TEM images of CUMS-Flx and CUMS-Alb).

We next isolated the total hippocampal lipids and performed targeted lipidomic analysis to quantify all the major membrane lipid species in rat hippocampus, including phospholipids, cholesterol, and sphingolipids. Five different phospholipid species, including PC, PE, PG, PA, ethanolamine plasmalogens (PIsEtn), and 2 subclasses of sphingolipids, including SM and Cer were measured. No significant differences were observed among the four tested groups on the total membrane lipids content, cholesterol, total phospholipids, and total sphingolipids (Fig. 3B-3E). Further analysis revealed the altered lipids subclasses in response to chronic stress and albiflorin treatment (Fig. 3F). Interestingly, we found that chronic stress resulted in a significant reduction of PC, PA, PIsEtn lipids, and SM in rat hippocampi. In contrast, PI, PE lipids, and Cer were increased dramatically after stress. The phospholipid perturbations in rat hippocampi were rapidly corrected by albiflorin treatment (Fig. 3F).

We then performed molecular docking analysis between albiflorin, and 5 key enzymes associated with phospholipid metabolism. Interestingly, out of 5 enzymes tested, cPLA2 had the lowest binding free energy of -132.8 kcal/mol (Fig. S7). As shown in Fig. 3G, albiflorin fits into

the active site of cPLA2 by forming hydrogen bonds with amino acid residues Ser 361, Gly 330, Leu 768, and Met 771 of cPLA2. cPLA2 is the key enzyme in membrane phospholipids metabolism through the production of arachidonic acid (AA, 20:4n-6) and other polyunsaturated free fatty acids, PUFAs) (Fig. 3H). In addition, the membrane can serve as the allosteric activators for cPLA2 in response to stress (Mouchlis et al., 2015). Based on these facts, we further analyzed the effects of albiflorin on cPLA2 through both in vitro enzymatic assay and in vivo CUMS rat model of depression. In vitro enzymatic assay showed that albiflorin is potential inhibitor of cPLA2 with the half maximal inhibitory concentration (IC_{50}) of 333.2 nM (Fig. 3I). Compared to the controls, chronic stress induced a significant increase of cPLA2 expression in rat hippocampi (Fig. 3J). This was corrected by albiflorin treatment in a dose-dependent manner (Fig. 3J). Downregulation of cPLA2 by albiflorin resulted in the increase of PC lipids and the decrease of eicosanoid levels such as PGF2 alpha and 20-HETE (Fig. 3K and 3L). Inhibition of cPLA2 also directed metabolic flow towards PE lipids catabolism for the generation of protective endocannabinoid anandamide (AEA), which was supported by upregulation of N-acyl phosphatidylethanolamine phospholipase D (NAPE-PLD) (Fig. 3M) and the increase of AEA in the hippocampus compared with CUMS rats treated with saline (CUMS-Alb versus CUMS-Sal) (Fig. 3N).

Inhibition of cPLA2 by albiflorin normalizes tryptophan metabolism via cPLA2-Akt1-IDO1 regulatory loop

IDO1 is the initial rate-limiting enzyme in tryptophan metabolism via the kynurenine pathway, and the hippocampus is a critical brain locus of IDO1 activity. In the CUMS rat model of depression, we found that the hippocampal expression of IDO1 was significantly upregulated under chronic stress (Fig. 4A). IDO1 expression was downregulated by albiflorin treatment in a dose-dependent manner (Fig. 4A). As a result of IDO1 inhibition, albiflorin corrected chronic

stress-induced increase of kynurenine (Kyn) /tryptophan (Trp) (Kyn/Trp) ratio in both rat plasma and hippocampus (Fig. 4B and 4C).

Additionally, we tested the inhibitory effects of albiflorin on IDO1 using LPS treated mice. Albiflorin reduced the increased levels of metabolites in the kynurenine pathway in the hippocampus of LPS-treated animals such as Kyn, 3-hydroxykynurenine (3-HK), and quinolinic acid (QUIN), which are the neurotoxins leading to neuronal death, inflammation, and depressive-like behaviors (Fig. 4D) (Stone and Darlington, 2002). However, such an effect was less remarkable in the fluoxetine treatment group. In addition, by inhibiting IDO1 activity, albiflorin diverted tryptophan metabolism towards serotonin biosynthesis. A significant increase in the hippocampal serotonin level in albiflorin treated animals was observed (Fig. 4E).

We next further explored how albiflorin inhibits IDO1 and thus corrects abnormal tryptophan metabolism. Albiflorin only showed weak direct inhibition of recombinant human IDO1 activity by in vitro enzymatic assay (IC_{50} > 100 μM) (Fig. 4F). Our previous analysis demonstrated that albiflorin is a strong inhibitor of cPLA2. The interplay between IDO1, protein kinase B (Akt1) , and cPLA2 had been reported by studies in cancers and human leukemia cells (Basu et al., 2006; Iachininoto et al., 2013). We then hypothesized that the inhibition of hippocampal IDO1 expression in tryptophan metabolism by albiflorin might be driven through inhibiting hippocampal cPLA2 activities. To confirm our hypothesis, we performed the protein-protein interaction (PPI) network analysis to investigate the interactions of IDO1 with other proteins (Fig. 4G). Surprisingly, we found that IDO1 is closely associated with Akt1, phosphatidylinositol 3 kinase (PI3K), and COX-2 (Fig. 4G and 4H). A recent study also found that constitutive IDO1 expression is dependent on cPLA2 and prostaglandins through PI3K-Akt-mTOR and protein kinase C (PKC)-glycogen synthase kinase 3 (GSK) signaling pathways in human tumor cells (Hennequart et al., 2017). We next analyzed the phosphorylation of the key proteins in this regulatory loop in rat hippocampus in response to chronic stress and albiflorin

treatment. Interestingly, we found that chronic stress resulted in the accumulation of prostaglandins and eicosanoids such as PGF2 alpha and 20-HETE, through the cPLA2-COX-2 pathway (Fig. 3K, 3L and Fig. 4H). Prostaglandins triggered the inhibition of the phosphorylation of GSK3β, Atk1, and p70S6K (mTOR signaling) and the subsequent activation of IDO1 by the downstream proteins and transcription factors such as β-catenin and ETS translocation variant 4 (ETV4) (Fig. 4H and 4I). In contrast, albiflorin treatment led to a significant reduction of cPLA2 expression and the levels of hippocampal prostaglandins (Fig. 3K, 3L and Fig. 4H). Subsequently, the phosphorylation of GSK3β, Atk1, and p70S6K (mTOR signaling) was significantly increased by albiflorin, which then reduced the hippocampal IDO1 expression and normalized abnormal tryptophan metabolism (Fig. 4H and 4I).

Discussion

Delayed clinical onset of classical antidepressants is associated with many negative consequences for patients with depression, such as psychosocial losses, relapse, and suicide (Tylee and Walters, 2007). Increasing evidence indicates that alternations in metabolism are the main drivers of depression (Mathew and Lijffijt, 2017). In this study, we showed that albiflorin produces rapid antidepressant-like effects in three different murine models of depression through the normalization of dysregulated phospholipid metabolism via inhibiting cPLA2 and the correction of tryptophan metabolism abnormalities through the cPLA2-Akt1-IDO1 regulatory loop. Our study demonstrated that natural products like albiflorin direct at dysregulated neurometabolism might be an exciting new approach for rapid treatment of depression through enabling metabolic reprogramming.

Metabolic abnormalities have been sparsely observed in patients with depression as well as depressive-like animal models (Gui et al., 2018; Yang et al., 2019). To our knowledge, this is the first comprehensive metabolomic study to systematically evaluate metabolic abnormalities in

the hippocampus in three animal models of depression. We demonstrated that hippocampal phospholipid and tryptophan metabolism are common metabolic pathways disturbed in OBX, LPS, and CUMS depression models. Metabolic dysregulations play a critical role in the pathogenesis, treatment resistance, and disease relapse of depression. These mechanisms constitute, therefore, potent targets for the treatment of depression. Targeting metabolic activities offers a wide range of therapeutic possibilities that are particularly applicable to depression. Depression is a rather heterogeneous disorder that dramatically limits the efficacy of current antidepressants (Herzog et al., 2018). One of the advantages of targeting metabolic pathways as a better strategy is that the disturbances of metabolic pathways are more evolutionarily conserved than gene and protein abnormalities. So far, this new strategy has been tested for the treatment of acute myeloid leukemia (Chapuis et al., 2019). Our study expanded the scope of such a strategy for antidepressant-like actions.

Lipids are major constituents of the brain and are critical for proper brain function. In this study, we found that the subclasses of sphingolipids (SMs and ceramides) and glycerophospholipids (PA, PC, PI, PE, PIsEtn, and PG) were significantly changed in response to chronic stress. The stress-induced alternations of lipids composition in the rat hippocampus fit with previous observations in rat prefrontal cortex after chronic stress exposure (Oliveira et al., 2015). Interestingly, the total lipids content and the sum levels of lipid super classes (total sphingolipids and total glycerophospholipids) were not affected, which indicated that sphingolipid subclasses imbalance with an increase in ceramide and decrease in SMs was catalyzed by sphingolipid modulating enzymes in a quantitative way (Gault et al., 2010). Similarly, the combination of decreased phospholipids and increased lysophospholipids in rat hippocampal tissues after chronic stress suggested the activation of phospholipase 2 (PLA2), which converted phospholipids into equal amount of lysophospholipids (Dennis, et al., 2011). The central discovery of our study is that albiflorin produces the primary therapeutic effects on

dysregulated hippocampal phospholipid metabolism via inhibiting the overexpression of cPLA2 expression. Phospholipid metabolism plays an increasingly recognized role in the neuronal function of the hippocampus (Miranda et al., 2019). For example, hippocampal phospholipids form lipid rafts which relay signals from the membrane to intracellular compartments or to other cells. In addition, hippocampal phospholipids regulate synaptic neurotransmission and plasticity by determining the localization and function of proteins in the cell membrane (Muller et al., 2015). cPLA2 is the key enzyme in the rate-limiting step of phospholipids signaling, which had been implicated in the mediation of long-term depression (Le et al., 2010). The cPLA2-COX-2 cascade is also known to produce a variety of lipid mediators such as eicosanoids involved in inflammation. In our study, we found the occurrence of hippocampal neuroinflammation indicated by the accumulation of eicosanoids in stressed rats, which was effectively controlled by albiflorin treatment, but not fluoxetine. Brain neuroinflammation was also observed in some patients with MDD (Setiawan et al., 2015). Currently, there is no FDA-approved drug for neuroinflammation. Although the clinical trials with nonsteroidal anti-inflammatory drugs (NSAIDs) showed encouraging results in improving depressive symptoms, the severe long-term side effects of NSAIDs such as liver toxicity can not be ignored (Kohler et al., 2014).

Inducible dysregulation of the tryptophan metabolism via kynurenine has been linked to several complex disorders, including depression (Cervenka et al., 2017). IDO is the rate-limiting key enzyme in this pathway. In our study, we found that albiflorin inhibits hippocampal IDO1 expression, likely through the interactions of cPLA2-COX2 and PI3K-Akt-mTOR signaling pathways. IDO1 inhibitors were extensively tested for the treatment of cancers as immunotherapy by a number of pharmaceutical companies (Sheridan, 2015). The versatile roles of IDO1 in the pathogenesis of many diseases highlight the concurrent treatment of depression and co-existing disorders through IDO1 inhibition. A previous study had demonstrated the

attenuation of both nociceptive and depressive behaviors in mice through the inhibition of hippocampal IDO1 activity with 1-methyl-D-tryptophan (Kim et al., 2012).

Even though the peony root extract is currently available in the market as a healthcare product, we did not recommend the unauthorized use of high doses of albiflorin to patients at this stage. Clinical trials are needed over the next several years at multiple sites.

In summary, our study demonstrated that albiflorin produces fast-acting antidepressant-like effects in OBX, LPS, and CUMS-induced murine models of depression. Using multi-omics approaches, we identified dysregulated hippocampal phospholipid and tryptophan metabolism across all three models, suggesting a common and conserved mechanism to depression. Moreover, we showed that albiflorin normalizes phospholipid metabolism through the inhibition of cPLA2 and corrects tryptophan metabolism via the cPLA2-Akt1-IDO1 regulatory loop. Our study, therefore, provides a novel therapeutic approach for the treatment of depression, thus resulting in a renaissance in the field of neurometabolism.

Author contribution

Y.L.C., Z.Z., and K.L. designed the research; Y.L.C., Q.S.W., K.Y., K.D.L., and L.N.G. conducted the experiments; Y.L.C., X.W., and Z.Z. contributed new reagents or analytical tools; Y.C., Q.S.W., K.Y., K.D.L., L.N.G., Z.Z., and K.L. analyzed the data. Y.L.C., Q.S.W., K.Y., L.N.G., and K.L. wrote the manuscript. All the authors discussed the results and commented on the manuscript. All data were generated in-house, and no paper mill was used. All authors agree to be accountable for all aspects of work ensuring integrity and accuracy.

Acknowledgments

This work was supported by grants from the National Natural Science Foundation of China (No. 81741119, 81628008), the Natural Science Foundation of Tianjin City (No. 16JCQNJC14400), and CAMS Innovation Fund for Medical Sciences (CIFMS, 2016-I2M-3-015).

Conflict of Interest

Z.Z is the co-founder of Beijing Wonner Biotech Co., Ltd., that is holding the US, Europe, and China patents for the use of albiflorin in the treatment of depression (China patent no. ZL2009102654220, ZL201180051467.3, ZL201080069710.X; US patent no. US9023817B2, US9453041B2, US20130231469A1, US20130316966 A1, US9555055B2 and Europe patent no. EP2491934B1). Other authors declare no competing interests.

Data availability statement

The metabolomic data were deposited at metabolomics workbench (Accession no. ST000903), and RNA-Seq data were deposited at Gene Expression Omnibus (GEO) (Accession no. SUB3179486).

References

Basu, G.D., Tinder, T.L., Bradley, J.M., Tu, T., Hattrup, C.L., Pockaj, B.A., Mukherjee, P., 2006. Cyclooxygenase-2 inhibitor enhances the efficacy of a breast cancer vaccine: role of IDO. J. Immunol. 177, 2391-2402.

Belmaker, R.H., Agam, G., 2008. Major depressive disorder. N. Engl. J. Med. 358, 55-68.

Berton, O., Nestler, E.J., 2006. New approaches to antidepressant drug discovery: beyond monoamines. Nat. Rev. Neurosci. 7, 137-151.

Blais, E.M., Rawls, K.D., Dougherty, B.V., Li, Z.I., Kolling, G.L., Ye, P., Wallqvist, A., Papin, J.A., 2017. Reconciled rat and human metabolic networks for comparative toxicogenomics and biomarker predictions. Nat. Commun. 8, 14250.

Cervenka, I., Agudelo, L.Z., Ruas, J.L., 2017. Kynurenines: Tryptophan's metabolites in exercise, inflammation, and mental health. Science 357, eaaf9794.

Chapuis, N., Poulain, L., Birsen, R., Tamburini, J., Bouscary, D., 2019. Rationale for targeting deregulated metabolic pathways as a therapeutic strategy in acute myeloid leukemia. Front Oncol. 9, 405.

Cui, S., Li, K., Ang, L., Liu, J., Cui, L., Song, X., Lv, S., Mahmud, E., 2017. Plasma phospholipids and sphingolipids identify stent restenosis after percutaneous coronary intervention. JACC Cardiovasc. Interv. 10, 1307-1316.

Dantzer, R., O'Connor, J.C., Freund, G.G., Johnson, R.W., Kelley, K.W., 2008. From inflammation to sickness and depression: when the immune system subjugates the brain. Nat. Rev. Neurosci. 9, 46-56.

de Bodinat, C., Guardiola-Lemaitre, B., Mocaer, E., Renard, P., Munoz, C., Millan, M.J., 2010. Agomelatine, the first melatonergic antidepressant: discovery, characterization and development. Nat. Rev. Drug Discov. 9, 628-642.

Dennis, E.A., Cao, J., Hsu, Y.H., Magrioti, V., Kokotos, G., 2011. Phospholipase A2 enzymes: physical structure, biological function, disease implication, chemical inhibition, and therapeutic intervention. Chem Rev 111, 6130-6185.

Drysdale, A.T., Grosenick, L., Downar, J., Dunlop, K., Mansouri, F., Meng, Y., Fetcho, R.N., Zebley, B., Oathes, D.J., Etkin, A., Schatzberg, A.F., Sudheimer, K., Keller, J., Mayberg, H.S., Gunning, F.M., Alexopoulos, G.S., Fox, M.D., Pascual-Leone, A., Voss, H.U., Casey, B.J., Dubin, M.J., Liston, C., 2017. Resting-state connectivity biomarkers define neurophysiological subtypes of depression. Nat. Med. 23, 28-38.

Duman, R.S., Aghajanian, G.K., Sanacora, G., Krystal, J.H., 2016. Synaptic plasticity and depression: new insights from stress and rapid-acting antidepressants. Nat. Med. 22, 238-249.

Duman, R.S., Voleti, B., 2012. Signaling pathways underlying the pathophysiology and treatment of depression: novel mechanisms for rapid-acting agents. Trends Neurosci. 35, 47-56.

Friedrich, M.J., 2017. Depression is the leading cause of disability around the world. JAMA 317, 1517.

Gault, C.R., Obeid, L.M., Hannun, Y.A., 2010. An overview of sphingolipid metabolism: from synthesis to breakdown. Adv Exp Med Biol 688, 1-23.

Gui, S.W., Liu, Y.Y., Zhong, X.G., Liu, X., Zheng, P., Pu, J.C., Zhou, J., Chen, J.J., Zhao, L.B., Liu, L.X., Xu, G., Xie, P., 2018. Plasma disturbance of phospholipid metabolism in major depressive disorder by integration of proteomics and metabolomics. Neuropsychiatr Dis. Treat. 14, 1451-1461.

Han, J., Xia, Y., Lin, L., Zhang, Z., Tian, H., Li, K., 2018. Next-generation metabolomics in the development of new antidepressants: using albiflorin as an example. Curr. Pharm. Des. 24, 2530-2540.

Harmer, C.J., Duman, R.S., Cowen, P.J., 2017. How do antidepressants work? New perspectives for refining future treatment approaches. Lancet Psychiatry 4, 409-418.

Harvey, A.L., Edrada-Ebel, R., Quinn, R.J., 2015. The re-emergence of natural products for drug discovery in the genomics era. Nat. Rev. Drug Discov. 14, 111-129.

He, D.Y., Dai, S.M., 2011. Anti-inflammatory and immunomodulatory effects of paeonia lactiflora pall., a traditional chinese herbal medicine. Front Pharmacol. 2, 10.

Hennequart, M., Pilotte, L., Cane, S., Hoffmann, D., Stroobant, V., Plaen, E., Van den Eynde, B.J., 2017. Constitutive IDO1 expression in human tumors is driven by cyclooxygenase-2 and mediates intrinsic immune resistance. Cancer Immunol. Res. 5, 695-709.

Herzog, D.P., Beckmann, H., Lieb, K., Ryu, S., Muller, M.B., 2018. Understanding and predicting antidepressant response: using animal models to move toward precision psychiatry. Front Psychiatry 9, 512.

Hu, X.L., Li, Y.B., Qi, S., Zhang, Q., Ren, T.S., Meng, W.H., Zhao, Q.C., 2016. 4-O-galloylalbiflorin discovered from Paeonia lactiflora Pall. is a potential beta-site amyloid precursor protein cleaving enzyme 1 (BACE1) inhibitor. J. Funct. Foods 27, 517-525.

Iachininoto, M.G., Nuzzolo, E.R., Bonanno, G., Mariotti, A., Procoli, A., Locatelli, F., De Cristofaro, R., Rutella, S., 2013. Cyclooxygenase-2 (COX-2) inhibition constrains indoleamine 2,3-dioxygenase 1 (IDO1) activity in acute myeloid leukaemia cells. Molecules 18, 10132-10145.

Jin, Z.L., Gao, N., Xu, W., Xu, P., Li, S., Zheng, Y.Y., Xue, M., 2016. Receptor and transporter binding and activity profiles of albiflorin extracted from *Radix paeoniae* Alba. Sci. Rep. 6, 33793.

Kim, H., Chen, L., Lim, G., Sung, B., Wang, S., McCabe, M.F., Rusanescu, G., Yang, L., Tian, Y., Mao, J., 2012. Brain indoleamine 2,3-dioxygenase contributes to the comorbidity of pain and depression. J. Clin. Invest. 122, 2940-2954.

Kohler, O., Benros, M.E., Nordentoft, M., Farkouh, M.E., Iyengar, R.L., Mors, O., Krogh, J., 2014. Effect of anti-inflammatory treatment on depression, depressive symptoms, and adverse effects: a systematic review and meta-analysis of randomized clinical trials. JAMA Psychiatry 71, 1381-1391.

Le, T.D., Shirai, Y., Okamoto, T., Tatsukawa, T., Nagao, S., Shimizu, T., Ito, M., 2010. Lipid signaling in cytosolic phospholipase A2alpha-cyclooxygenase-2 cascade mediates cerebellar long-term depression and motor learning. Proc. Natl. Acad. Sci. USA 107, 3198-3203.

Lee, S., Kim, H.B., Hwang, E.S., Kim, E.S., Kim, S.S., Jeon, T.D., Song, M.C., Lee, J.S., Chung, M.C., Maeng, S., Park, J.H., 2018. Antidepressant-like effects of p-coumaric acid on LPS-induced depressive and inflammatory changes in rats. Exp. Neurobiol. 27, 189-199.

Li, H., Ye, M., Zhang, Y., Huang, M., Xu, W., Chu, K., Chen, L., Que, J., 2015. Blood-brain barrier permeability of Gualou Guizhi granules and neuroprotective effects in ischemia/reperfusion injury. Mol. Med. Rep. 12, 1272-1278.

Li, J., Yang, Z., Qiu, H., Wang, Y., Jian, L., Ji, J., Li, K., 2020. Anxiety and depression among general population in China at the peak of the COVID-19 epidemic. World Psychiatry 19, 249-250.

Li, K., Wang, X., Pidatala, V.R., Chang, C.P., Cao, X., 2014. Novel quantitative metabolomic approach for the study of stress responses of plant root metabolism. J. Proteome Res. 13, 5879-5887.

Li, K., Wu, Y., Li, K., 2021. Be Prepared for a Mental Illness "Pandemic" in China: Too Early to Celebrate the Victory Over COVID-19. Disaster Med. Public Health Prep., 1-2.

Mathew, S.J., Lijffijt, M., 2017. Neurometabolic abnormalities in treatment-resistant depression. Am. J. Psychiatry 174, 3-5.

Mazza, M.G., Palladini, M., De Lorenzo, R., Magnaghi, C., Poletti, S., Furlan, R., Ciceri, F., group, C.-B.O.C.S., Rovere-Querini, P., Benedetti, F., 2021. Persistent psychopathology and neurocognitive impairment in COVID-19 survivors: Effect of inflammatory biomarkers at three-month follow-up. Brain Behav. Immun. 94, 138-147.

Miranda, A.M., Bravo, F.V., Chan, R.B., Sousa, N., Di Paolo, G., Oliveira, T.G., 2019. Differential lipid composition and regulation along the hippocampal longitudinal axis. Transl. Psychiatry 9, 144.

Mishra, B.B., Tiwari, V.K., 2011. Natural products: an evolving role in future drug discovery. Eur. J. Med. Chem. 46, 4769-4807.

Mouchlis, V.D., Bucher, D., McCammon, J.A., Dennis, E.A., 2015. Membranes serve as allosteric activators of phospholipase A2, enabling it to extract, bind, and hydrolyze phospholipid substrates. Proc. Natl. Acad. Sci. USA 112, E516-525.

Muller, C.P., Reichel, M., Muhle, C., Rhein, C., Gulbins, E., Kornhuber, J., 2015. Brain membrane lipids in major depression and anxiety disorders. Biochim. Biophys. Acta 1851, 1052-1065.

Murray, C.J., Lopez, A.D., 1997. Alternative projections of mortality and disability by cause 1990-2020: Global burden of disease study. Lancet 349, 1498-1504.

Oliveira, T.G., Chan, R.B., Bravo, F.V., Miranda, A., Silva, R.R., Zhou, B., Marques, F., Pinto, V., Cerqueira, J. J., Di Paolo, G., Sousa, N., 2016. The impact of chronic stress on the rat brain lipidome. Mol. Psychiatry 21, 80-88.

Pu, J., Yu, Y., Liu, Y., Tian, L., Gui, S., Zhong, X., Fan, C., Xu, S., Song, X., Liu, L., Yang, L., Zheng, P., Chen, J., Cheng, K., Zhou, C., Wang, H., Xie, P., 2020. MENDA: a comprehensive curated resource of metabolic characterization in depression. Brief Bioinform. 21, 1455-1464.

Ramaker, M.J., Dulawa, S.C., 2017. Identifying fast-onset antidepressants using rodent models. Mol. Psychiatry 22, 656-665.

Setiawan, E., Wilson, A.A., Mizrahi, R., Rusjan, P.M., Miler, L., Rajkowska, G., Suridjan, I., Kennedy, J.L., Rekkas, P.V., Houle, S., Meyer, J.H., 2015. Role of translocator protein density, a marker of neuroinflammation, in the brain during major depressive episodes. JAMA Psychiatry 72, 268-275.

Sheridan, C., 2015. IDO inhibitors move center stage in immuno-oncology. Nat. Biotechnol. 33, 321-322.

Shi, Y., Lin, P., Wang, X., Zou, G., Li, K., 2018. Sphingomyelin phosphodiesterase 1 (SMPD1) mediates the attenuation of myocardial infarction-induced cardiac fibrosis by astaxanthin. Biochem. Biophys. Res. Commun. 503, 637-643.

Stone, T.W., Darlington, L.G., 2002. Endogenous kynurenines as targets for drug discovery and development. Nat. Rev. Drug Discov. 1, 609-620.

Tylee, A., Walters, P., 2007. Onset of action of antidepressants. BMJ 334, 911-912.

van Hattum, H., Waldmann, H., 2014. Biology-oriented synthesis: harnessing the power of evolution. J. Am. Chem. Soc. 136, 11853-11859.

Vuong, H.E., Yano, J.M., Fung, T.C., Hsiao, E.Y., 2017. The Microbiome and Host Behavior. Annu. Rev. Neurosci. 40, 21-49.

Wang, Y.L., Wang, J.X., Hu, X.X., Chen, L., Qiu, Z.K., Zhao, N., Yu, Z.D., Sun, S.Z., Xu, Y.Y., Guo, Y., Liu, C., Zhang, Y.Z., Li, Y.F., Yu, C.X., 2016. Antidepressant-like effects of albiflorin extracted from *Radix paeoniae* Alba. J. Ethnopharmacol. 179, 9-15.

Yang, L.N., Pu, J.C., Liu, L.X., Wang, G.W., Zhou, X.Y., Zhang, Y.Q., Liu, Y.Y., Xie, P., 2019. Integrated metabolomics and proteomics analysis revealed second messenger system disturbance in hippocampus of chronic social defeat stress rat. Front Neurosci. 13, 247.

Yuan, M., Breitkopf, S.B., Yang, X., Asara, J.M., 2012. A positive/negative ion-switching, targeted mass spectrometry-based metabolomics platform for bodily fluids, cells, and fresh and fixed tissue. Nat. Protoc. 7, 872-881.

Zhang, H., Li, K., Zhao, Y., Zhang, Y., Sun, J., Li, S., Lin, G., 2020. Long-term use of fluoxetine accelerates bone loss through the disruption of sphingolipids metabolism in bone marrow adipose tissue. Transl. Psychiatry 10, 138.

Zhao, Z.X., Fu, J., Ma, S.R., Peng, R., Yu, J.B., Cong, L., Pan, L.B., Zhang, Z.G., Tian, H., Che, C.T., Wang, Y., Jiang, J.D., 2018. Gut-brain axis metabolic pathway regulates antidepressant efficacy of albiflorin. Theranostics 8, 5945-5959.

Figures

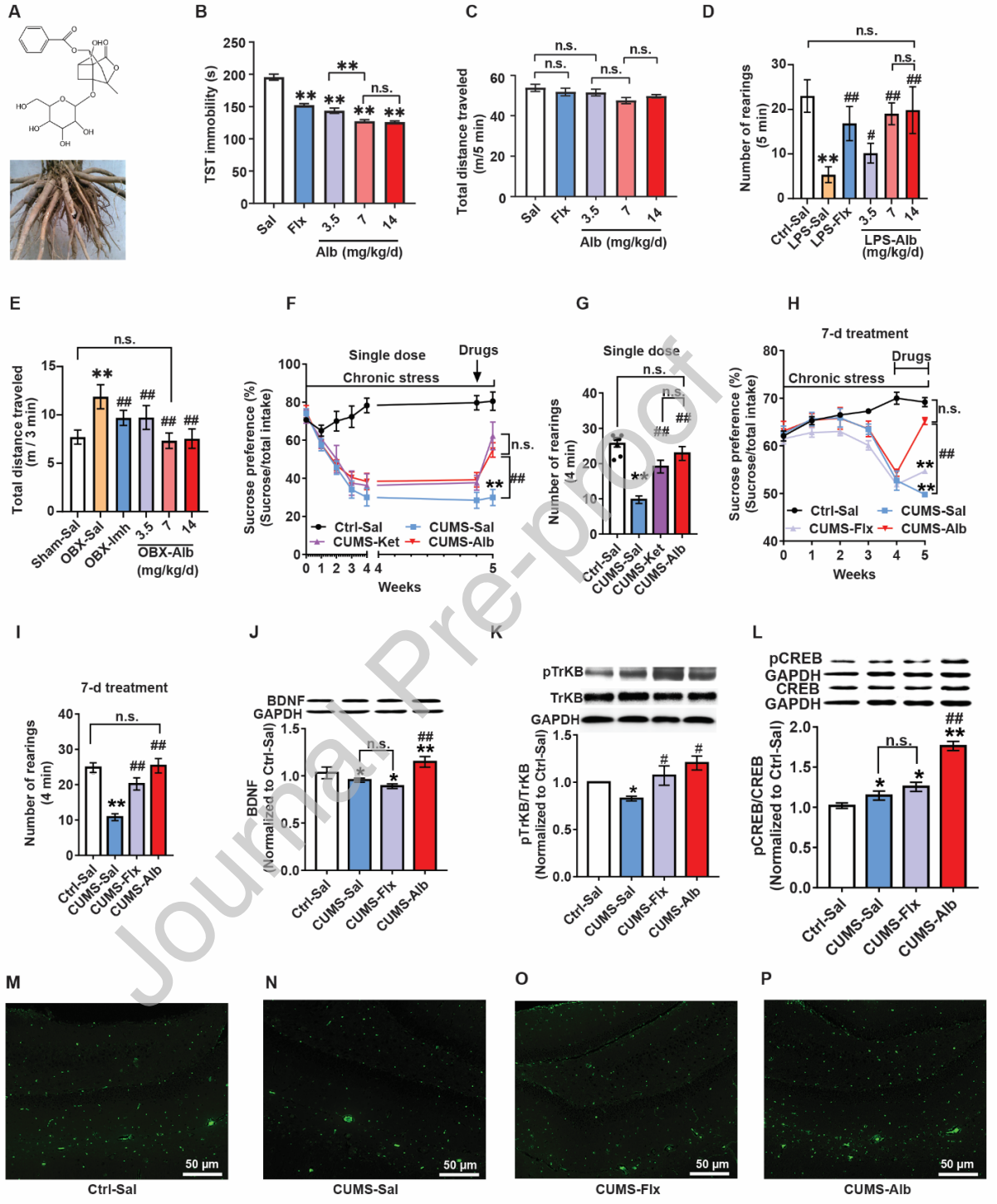

Fig. 1. Albiflorin produces fast-onset antidepressant-like effects in three murine models of depression. (A) Albiflorin (Alb) isolated from Peony roots. **(B)** The time of immobility in mice was

significantly decreased by albiflorin in a dose-dependent manner in tail suspension test (TST) (Data were mean ± SEM, N = 12 rat/group, One-way analysis of variance (ANOVA) with Tukey's test, $^{**}P < 0.01$ vs. saline group, n.s. not significant). (**C**) Albiflorin treatment did not significantly alter the spontaneous activity of mice, as shown by the unchanged total distance traveled by rat within 5 min in the open field test (OFT). (Data were mean ± SEM, N = 12 rat/group, One-way ANOVA with Tukey's test, n.s. not significant). **(D)** LPS-induced mice hypolocomotion in OFT was normalized by albiflorin treatment. (Data were mean ± SEM, N = 12 mice/group, ANOVA with Tukey's test, $^{**}P < 0.01$ vs Ctrl-Sal and $^{\#\#}P < 0.01$ vs LPS-Sal). **(E)** Olfactory bulbectomy (OBX)-induced hyperactivity was completely normalized by albiflorin. (Data were mean ± SEM, N = 12 rats/group, ANOVA with Tukey's test, $^{*}P < 0.05$ and $^{**}P < 0.01$ vs Sham-Sal; $^{\#}P < 0.05$ vs OBX-Sal). (**F**) A single dose of albiflorin (7 mg/kg) corrected the reduction of sucrose preference caused by chronic stress. (Data were mean ± SEM, N = 8 rats/group, One-way ANOVA with Tukey's test, $^{**}P < 0.01$ vs Ctrl-Sal and $^{\#\#}P < 0.01$ vs CUMS-Sal). (**G**) Similar to ketamine (Ket), one dose of albiflorin (7 mg/kg) corrected the significant reduction of rearings caused by chronic stress in OFT. (Data were mean ± SEM, N = 8 rats/group, One-way ANOVA with Tukey's test, $^{**}P < 0.01$ vs Ctrl-Sal and $^{\#\#}P < 0.01$ vs CUMS-Sal). **(H)** Treatment with albiflorin (7 mg/kg/d) for 7 days resulted in a significant increase of sucrose preference in chronically stressed rats. (Data were mean ± SEM, N = 8 rats/group, one-way ANOVA with Tukey's test, $^{**}P < 0.01$ vs Ctrl-Sal and $^{\#\#}P < 0.01$ vs CUMS-Sal). (**I**) The decrease of rearings in chronically stressed rats was normalized by 7 days of albiflorin treatment. (Data were mean ± SEM, N = 8 rats/group, ANOVA with Tukey's test, $^{**}P < 0.01$ vs Ctrl-Sal and $^{\#\#}P < 0.01$ vs CUMS-Sal). **(J-L)** Albiflorin treatment for 7 days significantly increased the expression of proteins associated with antidepressant-onset including BDNF, pTrKB and pCREB (Data were mean ± SD, N = 3 independent experiments, $^{*}P < 0.05$ and $^{**}P < 0.01$ vs Ctrl-Sal, $^{\#}P < 0.05$ and $^{\#\#}P < 0.01$ vs CUMS-Sal). **(M-P)** Albiflorin treatment increased rat hippocampal cell proliferation revealed by proliferating cell nuclear antigen (PCNA) immunostaining. Scale bar = 50 μm.

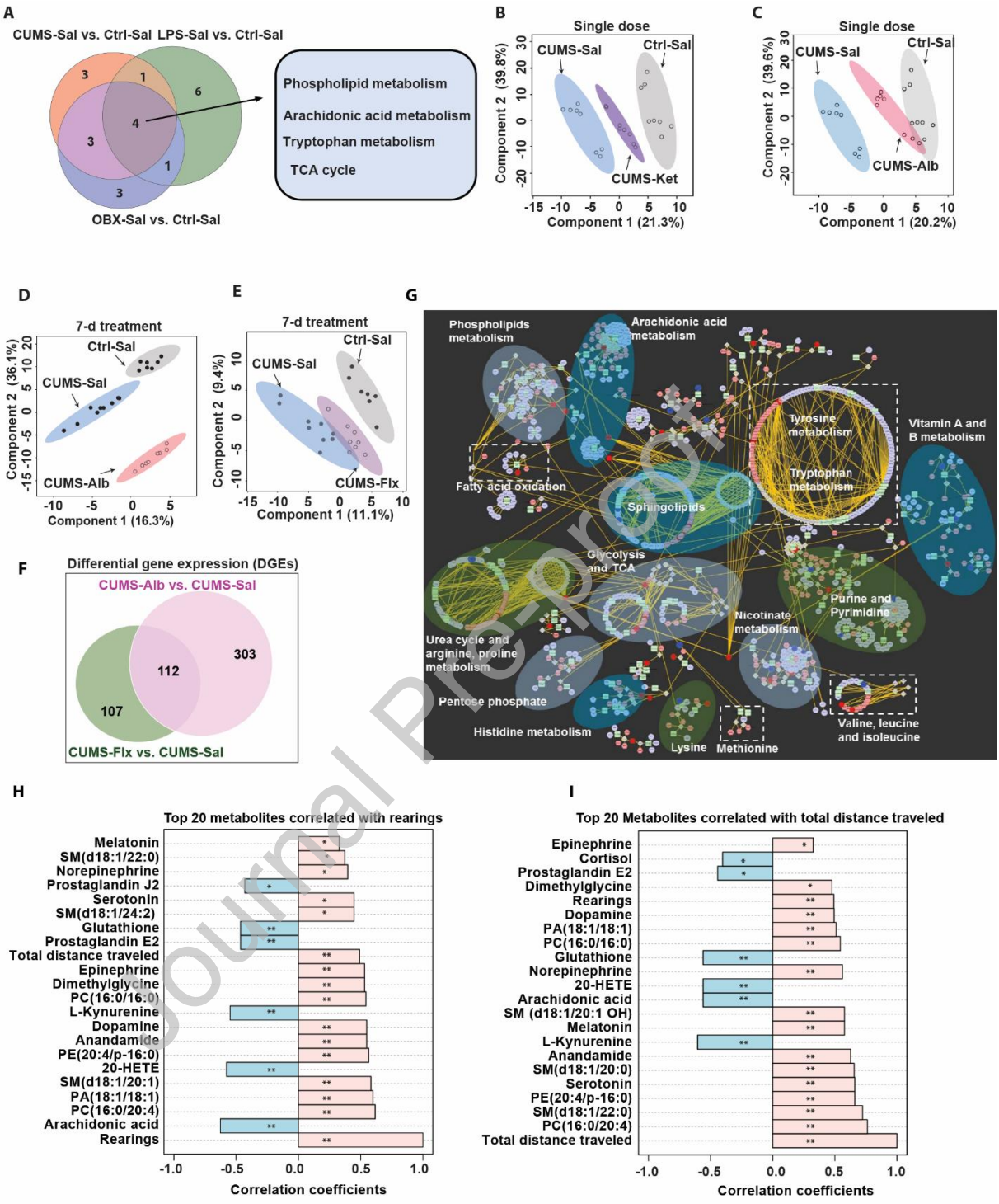

Fig. 2

Fig. 2. The rapid antidepressant-like effects of albiflorin are highly associated with the normalization of metabolic dysregulation in hippocampal phospholipid and tryptophan

metabolism in three models of depression. (A) Venn diagram of significantly altered hippocampal metabolic pathways that were in common or unique to three depression models. (**B-C**) Partial least square analysis (PLS-DA) revealed both a single dose of ketamine (**B**) and albiflorin (**C**) led to the complete separation of hippocampal metabolism from chronically stressed rats, while the albiflorin-treated group was much closer to the normal controls (N = 8 rats/group). (**D-E)** Severn days of albiflorin (7 mg/kg/d) treatment resulted in the complete separation of hippocampal metabolism from chronically stressed rats (**D**), while the partial restoration was observed by fluoxetine (Flx) treatment (**E**). (N =8 rats/group). (**F**) Venn diagram displayed the number of common and unique differentially expressed genes (DEGs) in the hippocampus between stressed rats treated with drugs and saline (N = 3 rats/group). (**G**) The integrated metabolomic and transcriptomic network analysis revealed the alternation of metabolic pathways in the hippocampus by albiflorin treatment. Nodes with hexagon shapes are metabolites, and circular nodes are genes. Blue nodes indicated significant downregulation, and red nodes indicated significant upregulation. (**H**) The top 20 hippocampal metabolites correlated with the improvement of rearing behaviors in CUMS rats after albiflorin treatment. (**I**) The top 20 hippocampal metabolites correlated with the increase of locomotor activities (total distance traveled) in CUMS rats after albiflorin treatment. Spearman's rank correlation, N = 8 rats/group, $^{**}P < 0.01$, $^{*}P < 0.05$ and false discovery rate (FDR) < 2%.

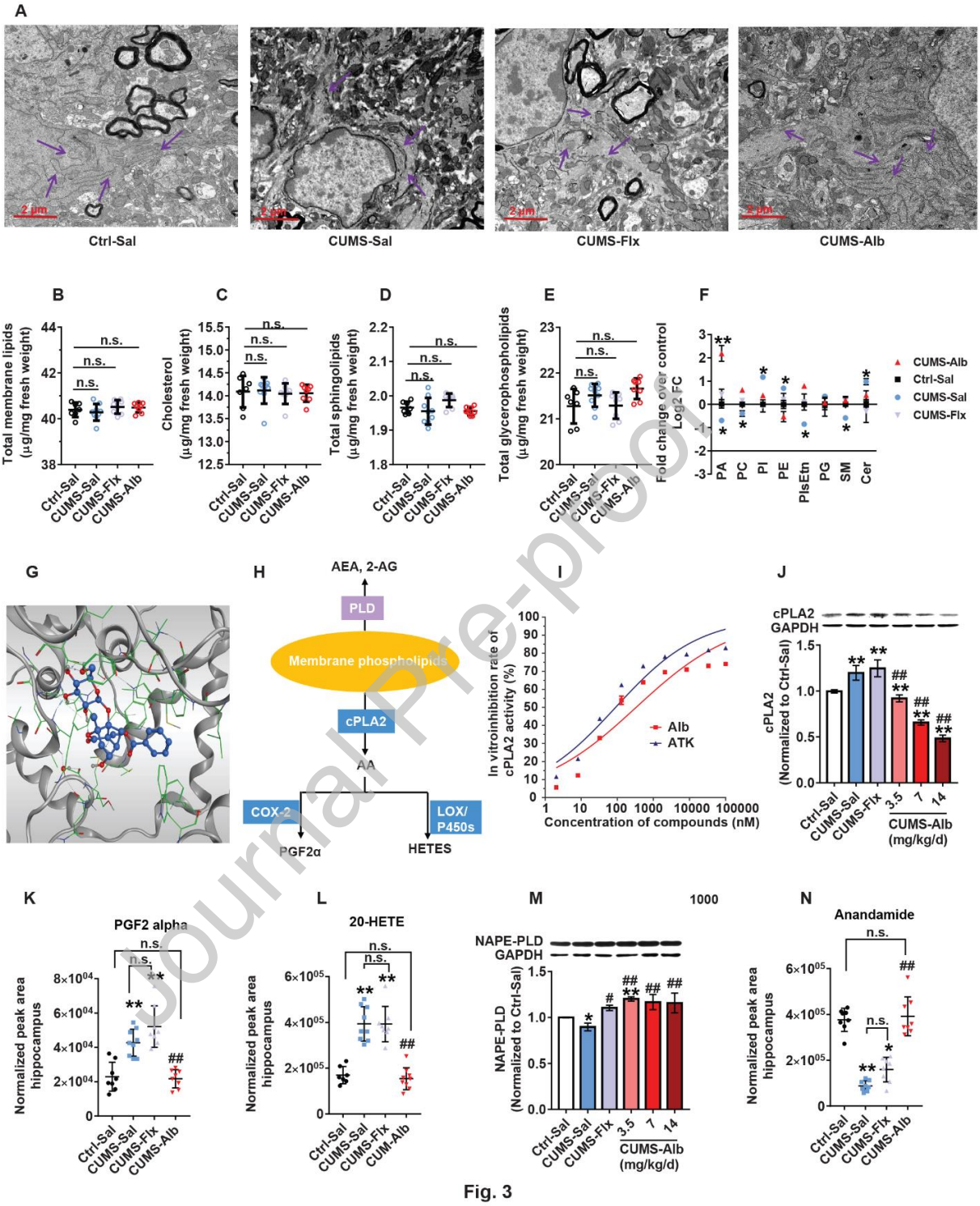

Fig. 3

Fig. 3. Albiflorin restores hippocampal phospholipid homeostasis through inhibiting cPLA2. (A) Transmission electron microscope (TEM) images showed the restoration of cell membrane lipid bilayers in rat hippocampus by albiflorin. (Magnification: 15,000×). (**B-F)** Quantification of changes of rat

hippocampal total membrane lipids (**B**), cholesterol (**C**), total sphingolipids (**D**), total glycerophospholipids (**E**), and subclasses of glycerophospholipids (**F**) in response to chronic stress and albiflorin treatment. (Data were mean ± SD, N = 8 rats/group, Kruskal-Wallis with Dunn's test. $^{*}P < 0.05$ and $^{**}P < 0.01$ vs Ctrl-Sal. n.s: not significant). (**G**) The binding of albiflorin to the active site of the cPLA2 protein. Albiflorin was displayed in a ball and stick representation. Heteroatoms were colored as follows: green (carbon), red (oxygen), and gray (hydrogen). (**H**) A sketch diagram of the arachidonic acid cascade. (**I**) *In vitro* assay for the inhibition of the Cpla2 enzyme by albiflorin (N = 3 replicates/concentration). Arachidonyl trifluoromethyl ketone (ATK) a known cPLA2 inhibitor was used as the positive control. IC_{50} was calculated based on a non-linear regression model. (**J**) Albiflorin treatment led to the inhibition of cPLA2 expression in rat hippocampus. (Data were mean ± SD, N = 3 independent experiments, ANOVA with Tukey's test, $^{**}P < 0.01$ vs Ctrl-Sal, $^{\#\#}P < 0.01$ vs CUMS-Sal). (**K**) and (**L**) Albiflorin treatment led to the decrease of PGF2alpha (**K**) and 20-HETE (**L**) (Data were mean ± SD, N = 8 rats/group, ANOVA with Tukey's test. $^{**}P < 0.01$ vs Ctrl-Sal, $^{\#\#}P < 0.01$ vs CUMS-Sal, n.s.: not significant). (**M**) The significant upregulation of NAPE-PLD expression in rat hippocampus in response to albiflorin treatment (Data were mean ± SD, N = 3 independent experiments, ANOVA with Tukey's test, $^{*}P < 0.05$ and $^{**}P < 0.01$ vs Ctrl-Sal, $^{\#}P < 0.05$, $^{\#\#}P < 0.01$ vs CUMS-Sal, n.s.: not statistically significant). (**N**) Albiflorin treatment resulted in an increase of anandamide in the hippocampus. (Data were mean ± SD, N = 8 rats/group, ANOVA with Tukey's test. $^{*}P < 0.05$ and $^{**}P < 0.01$ vs Ctrl-Sal, $^{\#\#}P < 0.01$ vs CUMS-Sal, n.s.: not significant).

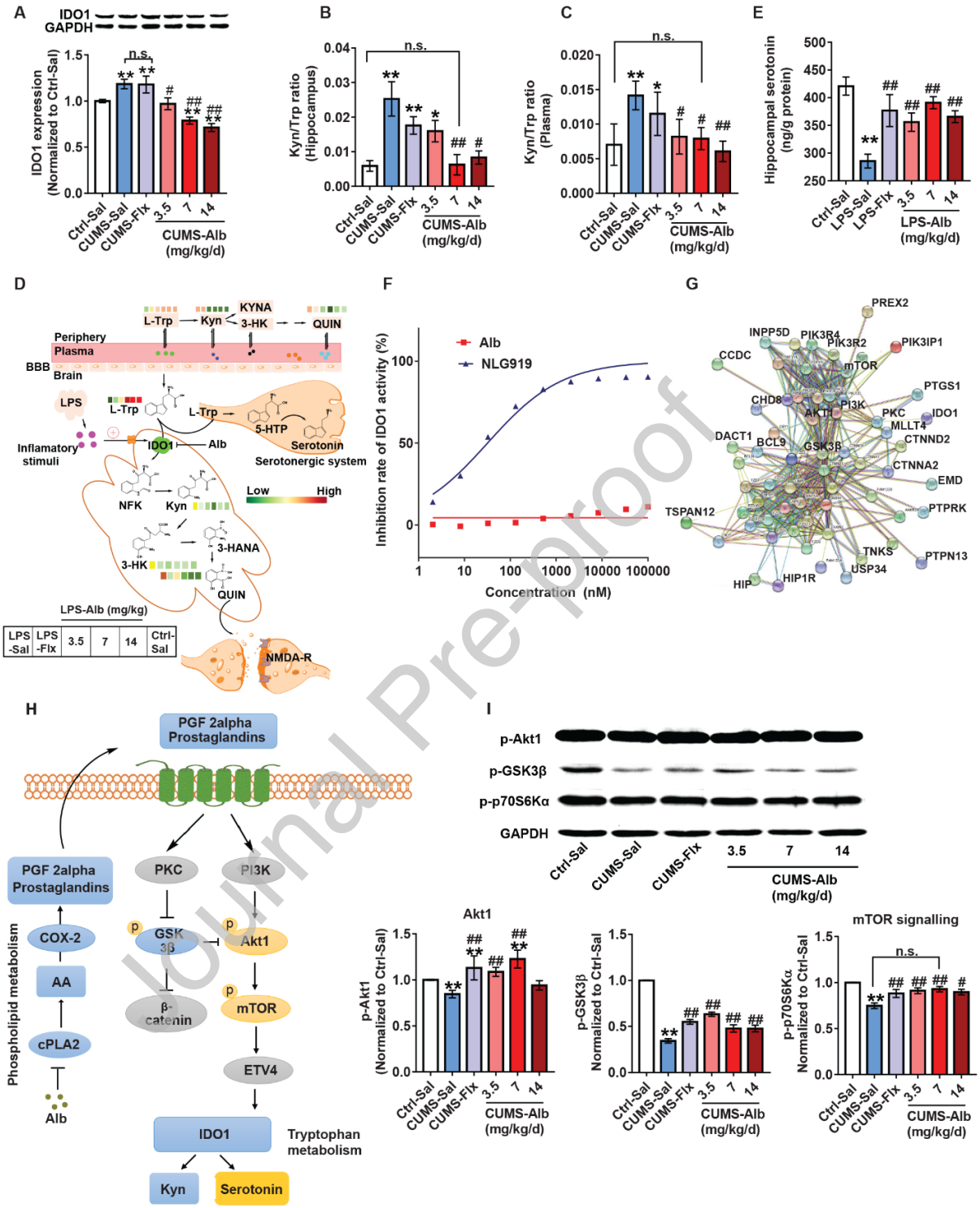

Fig. 4. Albiflorin normalizes the imbalanced kynurenine pathway of tryptophan metabolism in the hippocampus through the cPLA2-Akt1-IDO1 regulatory loop. (**A**) Albiflorin inhibited the

overexpression of IDO1 induced by chronic stress in the rat hippocampus. (Data were mean ± SEM, N = 3 independent experiments, $^{**}P < 0.01$ vs Ctrl-Sal, $^{\#}P < 0.05$, $^{\#\#} P < 0.01$ vs CUMS-Sal, n.s.: not statistically significant). (**B-C**) Albiflorin attenuated the stress-induced increase of kynurenine (Kyn) /tryptophan (Trp) ratio in both rat hippocampus (**B**) and plasma (**C**). (Data were mean ± SD, N = 8 rats/group, ANOVA with Tukey's test, $^{*}P < 0.05$ and $^{**}P < 0.01$ vs Ctrl-Sal, $^{\#}P < 0.05$ and $^{\#\#}P < 0.01$ vs CUMS-Sal. n.s. not significant). (**D**) Albiflorin inhibited the kynurenine pathway of tryptophan metabolism in an LPS-induced mouse model of depression. The color of metabolites was assigned based on their average concentrations (N = 8 mice/group) from green (lowest) to red (highest). (**E**) Albiflorin treatment resulted in a significant increase in hippocampal serotonin in LPS-stressed rats. (Data were mean ± SD, N = 8 mice/group, ANOVA with Tukey's test, $^{**}P < 0.01$ vs Ctrl-Sal, $^{\#\#}P < 0.01$ vs CUMS-Sal). (**F**) *In vitro* assay for the inhibition of the IDO1 enzyme by albiflorin (N = 3 replicates/concentration, NLG919, a known potent IDO1 inhibitor was used as the positive control. IC_{50} was calculated based on a non-linear regression model). **(G)** Protein-protein interactions of IDO1. The interaction network was obtained and visualized by STRING 11.0. (**H**) Changes of hippocampal protein expression in response to albiflorin treatment in the signal pathway of the cPLA2-COX-2-IDO1 regulatory loop. (Yellow color indicated upregulation after albiflorin treatment, and blue color indicated downregulation or decrease. Gray indicated not measured in this study. The symbol of p indicated the phosphorylation of the protein. The relative expression was mean ± SD, N = 3 independent experiments, $^{**}P < 0.01$ vs Ctrl-Sal and $^{\#\#}P < 0.01$ vs CUMS-Sal. n.s. not significant). Abbreviations: COX-2: Cyclooxygenase-2; GSK3β: Glycogen synthase kinase 3; Akt: Protein kinase B; mTOR: The mechanistic target of rapamycin; ETV4: ETS translocation variant 4; IDO1: Indoleamine 2, 3-dioxygenase 1; PI3K: Phosphoinositide 3-kinase and PKC: Protein kinase C.

List of Supplemental Materials

Supplemental Methods

Fig. S1. Additional behavioral tests for the rapid antidepressant-like effects of albiflorin in LPS-induced mice model of depression.

Fig.S2. Albiflorin treatment (7 mg/kg/d) for 7 days resulted in the increase of rat hippocampal neurogenesis in rats exposed to chronic stress.

Fig.S3. The pharmacokinetic behaviors of albiflorin in rat hippocampus and plasma.

Fig.S4. Assessment of partial least square discriminant analysis (PLS-DA) model for discriminating the hippocampal metabolomic features.

Fig.S5. Volcano plots showing the differential metabolites and genes in the hippocampus between the chronically stressed rats treated with drugs and saline.

Fig.S6. The differential metabolites in the plasma of chronically stressed rats and enriched pathways in response to albiflorin treatment compared to saline.

Fig.S7. The molecular docking between albiflorin and five key enzymes related to phospholipid metabolism.

Table S1. Pathways disturbed in rat hippocampus of olfactory bulbectomy (OBX)-induced rat model depression.

Table S2. Pathways disturbed by 35-day of chronically unpredicted mild stress (CUMS) in rat hippocampus compared to the normal control group.

Table S3. Pathways disturbed by lipopolysaccharide (LPS) in mice hippocampus compared to the normal control group.

Table S4. The top 14 metabolic pathways in rat hippocampus restored by albiflorin or fluoxetine treatment in CUMS model.

Table S5. Reagents, chemicals, antibodies, HPLC columns, and other critical resources used in this study.

Credit Author Statement

Y.L.C., Z.Z., and K.L. designed the research; Y.L.C., Q.S.W., K.Y., K.D.L., and L.N.G. conducted the experiments; Y.L.C., X.W., and Z.Z. contributed new reagents or analytical tools; Y.C., Q.S.W., K.Y., K.D.L., L.N.G., Z.Z., and K.L. analyzed the data. Y.L.C., Q.S.W., K.Y., L.N.G., and K.L. wrote the manuscript. All the authors discussed the results and commented on the manuscript. All data were generated in-house, and no paper mill was used. All authors agree to be accountable for all aspects of work ensuring integrity and accuracy.